Temperature and Anharmonic Effects on the Infrared Absorption Spectrum from a Quantum Statistical Approach: Application to Naphthalene

M. Basire,[†] P. Parneix,*[,†] F. Calvo,[‡] T. Pino,[†] and Ph. Bréchignac[†]

Laboratoire de Photophysique Moléculaire, CNSR, Université Paris-Sud, Bât. 210, F91405 Orsay Cedex, France, and LASIM, Université Claude Bernard Lyon I and UMR 5579, CNRS, Bât A. Kastler, 43 Bd du 11 Novembre 1918, F69622 Villeurbanne Cedex, France

Received: February 6, 2009; Revised Manuscript Received: April 28, 2009

A method is developed to calculate the finite-temperature infrared absorption spectrum of polyatomic molecules with energy levels described by a second-order Dunham expansion. The anharmonic couplings are fully incorporated in the calculation of the quantum density of states, achieved using a Wang−Landau Monte Carlo procedure, as well as in the determination of transition energies. Additional multicanonical simulations provide the microcanonical absorption intensity as a function of both the absorption wavelength and the internal energy of the molecule. The finite-temperature spectrum is finally obtained by Laplace transformation of this microcanonical histogram. The present scheme is applied to the infrared spectrum of naphthalene, for which we quantify the shifting, broadening, and third-order effects as a continuous function of temperature. The influence of anharmonicity and couplings is manifested on the nontrivial variations of these features with increasing temperature.

I. Introduction

Infrared (IR) spectroscopy has become a very powerful method to unravel the structural assignment of polyatomic species in the gas phase. Laboratory techniques based on Fourier transform infrared (FTIR) spectroscopy, IR depopulation, IR/UV, IR multiphoton dissociation (IRMPD), or messenger tagging, together with quantum chemical calculations, have allowed increasingly large systems to be unambiguously identified in the fields of bare neutral[1] or ionic[2–4] molecules, hydrogen-bonded complexes,[5–8] semiconductor[9] or metal[10] clusters, peptides,[11–19] and hydrocarbon molecules[20–26] including aromatic compounds.[27–33] The latter systems, especially the polycyclic aromatic hydrocarbons (PAHs), have been the subject of intense research in the recent decades due to their relevance in soots and combustion processes.[34,35] They are also presumed to exist in several astrophysical environments ranging from solar system bodies to the interstellar medium (ISM) of galaxies,[36–38] as suggested by infrared spectroscopy measurements in Space and the coincidence between the so-called aromatic infrared bands (AIBs) and the features observed for natural polycyclic aromatics.[39,40] The photophysical mechanisms of large hydrocarbon molecules in the interstellar environment have been discussed by various authors,[36–39] especially in relation with the competition between fluorescence and fragmentation resulting from starlight absorption.

One key issue in interpreting experimental IR spectra for molecules in hot media lies in the understanding of temperature effects on the vibrational bands.[20,41,42] Temperature essentially influences the band shapes and intensities through the anharmonicities of the potential energy surface (PES), but the vibrational dynamics is affected as well. In the case of PAHs, such effects have been measured in absorption,[43] and they have been occasionally reported in emission as well.[20–23,25,26] Temperature effects have been tentatively included in models of astro-PAH emission in Space in order to understand their role on the band profiles of the AIBs.[44–47] In the case of IRMPD measurements, similar models have highlighted how anharmonicities affect the intensity ratios and band profiles.[42] However, with the notable exception of the work by Mulas and coworkers,[47] anharmonicities in these models have been treated as parameters or taken from experiment rather than from a detailed description of the PES.

From the theoretical point of view, calculating infrared vibrational spectra that take temperature and anharmonic effects into account can be achieved using several methods, which span many orders of complexity. At the most basic level, harmonic frequencies obtained from a static quantum chemical calculation are scaled a posteriori in an ad hoc fashion in order to correct for basis set uncompleteness, approximations in the treatment of electron correlation, and basin anharmonicities.[48] Explicit molecular dynamics simulations fully incorporate anharmonicities and provide the infrared spectrum upon Fourier transformation of the electric dipole time-autocorrelation function. This rather general approach is most conveniently applied when the electronic ground-state potential energy surface is known beforehand and can be parametrized with force fields[49] or semiempirical models,[50,51] making it particularly suitable for relatively large systems. For molecules containing no more than a dozen atoms, energy surfaces generated on-the-fly, either with the Car−Parrinello[4,52] or with related schemes,[53] or by using Born−Oppenheimer molecular dynamics[54] have also been employed in this context. Finally, the classical approximation for the nuclear motion can be dealt with using path-integral-based techniques, sometimes even in conjunction with on-the-fly surfaces.[55–57] Small molecules, or systems for which the vibrational modes of interest allow some classical/quantum decoupling, also allow a more realistic quantum mechanical treatment of nuclear wave functions using the vibrational self-consistent field method[58] and some of its extensions.[59] Finally,

* To whom correspondence should be addressed. E-mail: pascal.parneix@u-psud.fr.
[†] Université Paris-Sud and UPR 3361.
[‡] Université Claude Bernard Lyon I and UMR 5579.

10.1021/jp901104x CCC: $40.75
Published on Web 05/28/2009

more approximate approaches such as the vibrational exciton model[60] provide some ways of estimating infrared spectra in much larger systems.

Alternatively, temperature effects on infrared spectra are, in principle, contained in the higher-order Dunham expansion of the energy in terms of the vibrational levels, through at least two effects. First, the transition energies, which only depend on the mode frequency in harmonic systems, carry some additional dependence with the vibrational state in anharmonic systems. Second, the equilibrium spectrum at some finite temperature depends on the population of vibrational states, which is related to the microcanonical density of vibrational states. Densities of states are notoriously difficult to calculate for polyatomic molecules, and the problem has been satisfactorily solved only for separable oscillators.[61,62] The added combinatorial complexity arising from couplings must be addressed at the computational level, using either partly approximate methods based on classical densities,[63–66] inverse Laplace transformation from quantum partition functions,[67] or direct Monte Carlo (MC) integration.[68,69] All of these approaches have various intrinsic limitations which make them poorly efficient in large systems. In particular, MC sampling of the quantum numbers space becomes harder due to an increasing variance.[70] In contrast, the Wang−Landau method[71] is particularly suitable in high-dimensional spaces,[72] and we have shown in a recent work how it can be used to calculate very accurate vibrational state densities for large, nonseparable systems.[73] Here, we extend the method for computing other energy-resolved quantities, which subsequently allows the calculation of infrared spectra at finite temperature. The present method thus entirely relies on static ingredients and provides anharmonic spectra without most approximations nor any fitted or empirical parameter.

Naphthalene was chosen as a first testing ground. The IR spectroscopy of this molecule has been characterized experimentally using matrix isolation techniques[74,75] and in vacuum,[20–23,31,32,41,43] as well as theoretically at first-principle[76–78] and semiempirical[50,51] levels. In addition, a fully coupled anharmonic potential energy surface for this molecule has recently been derived by Cané and co-workers[79] based on density functional theory calculations. The infrared spectra inferred here from these data are sufficiently accurate for permitting shape analyses in terms of spectral shifts and broadenings as a continuous function of temperature.

In the next section, we describe the simulation details for calculating the microcanonical density of states and the absorption spectrum at finite temperature. In section III, we describe the application to naphthalene, and section IV gives some concluding remarks.

II. Methods Section

In the present work, the absorption spectrum $I(\nu,T)$ at finite temperature is obtained from the corresponding spectrum in the microcanonical ensemble, $I(\nu,E)$, after a Laplace transformation. The computation of $I(\nu,T)$ is carried out in three steps. (i) We start by calculating the density of vibrational states, $\Omega(E)$; (ii) we accumulate the two-dimensional histogram $\mathcal{J}(\nu,E)$ of the intensity of transitions at frequency ν and internal energy E; and (iii) the microcanonical absorption spectrum $I(\nu,E)$ is simply the normalized value of $\mathcal{J}(\nu,E)$, and the canonical spectrum directly derives from it.

We consider a molecular system for which the structural details are known at the equilibrium structure. Besides the geometry, the harmonic vibrational frequencies $\{\nu_i\}$ and the anharmonic coefficients $\{\chi_{ij}\}$ are available, as obtained, for example, from quantum chemistry calculations.[80] The total energy E of the system, in the energy range of the present study, is expressed as a function of the m quantum numbers $\{n\} = n_1,\ldots, n_m$ as a Dunham expansion

$$E(\{n\}) = \sum_{i=1}^{m} h\nu_i\left(n_i + \frac{1}{2}\right) + \sum_{1\le i\le j\le m} \chi_{ij}\left(n_i + \frac{1}{2}\right)\left(n_j + \frac{1}{2}\right) \quad (1)$$

A. Anharmonic Densities of States. Quantum densities of vibrational states can be obtained exactly for sets of separable oscillators.[61,62] There are no such methods available when the oscillators are coupled but only approximate schemes.[63–66,68,69] Following our recent work,[73] we use the Wang−Landau method[71] to calculate the density of vibrational states of fully coupled oscillators with quadratic energy levels as in eq 1. Briefly, the method belongs to the "flat-histogram" Monte Carlo class and consists of performing a random walk in the space of quantum numbers $\{n\}$ and modifies a running estimate of the density of states $g(E)$ on-the-fly by penalizing each newly visited state.

In practice, the calculation is performed in a fixed energy range $[E_{\min},E_{\max}]$, and $g(E)$ is initially set to one in this entire range. From the current set $\{n\}_{\text{old}}$ of vibrational states with energy E_{old}, a new set $\{n\}_{\text{new}}$ is randomly generated by moving each quantum number n_i by $+1$, -1, or 0 with probability p, p, and $1 - 2p$, respectively. The precise value of p is optimized by comparison with the (separable) harmonic case, for which the exact density of states is known.[61] The trial configuration $\{n\}_{\text{new}}$ with energy E_{new} is accepted with a pseudo Metropolis rule,[71] but more importantly, the function g is modified by $g(E) \rightarrow g(E) \times f$, where the modification factor f is strictly higher than 1 but slowly decreases as the simulation proceeds. As f progressively tends to 1, g converges to the true density of states.

While many improvements to the Wang−Landau method have been proposed in the past,[72,81–87] we found that the original version was satisfactory enough for our purposes. In particular, and contrary to our previous calculation,[73] which required two independent Wang−Landau simulations on overlapping energy ranges in order to improve the accuracy at both ends, we were able to use a single window in our present implementation. For this, the vibrational quantum number n_k was restricted to be lower than an upper limit $n_k^{\max}$ chosen such that the associated mode energy $E_k = h\nu_k(n_k + 1/2) + \chi_{kk}(n_k + 1/2)^2$ remains in the increasing region. We checked on various observables (primarily the distributions of quantum numbers) that the sampling was not affected by this restriction.

B. Energy-Dependent Absorption Spectrum. We now consider the absorption properties of the set of coupled oscillators characterized by eq 1. For a given mode k, the intensity of the elementary transition between n_k and n_{k+1} is taken to be proportional to the absorption cross section $\sigma^{(k)}_{n_k\rightarrow n_{k+1}}$, which we estimate using a harmonic approximation as

$$\sigma^{(k)}_{n_k\rightarrow n_{k+1}} = (n_k + 1) \times \sigma^{(k)}_{0\rightarrow 1} \quad (2)$$

The coefficients $\sigma^{(k)}_{0\rightarrow 1}$ are assumed to be available as the result of quantum chemical calculations at the vibrational ground-state structure. This approximation is considered to be valid as long as anharmonicities are small. In that case, the vibrational wave functions are assumed to be harmonic, implying that eq 2 is still valid.

The energy difference $\Delta E^{(k)}$ associated with the transition $n_k \rightarrow n_{k+1}$ straightforwardly follows from eq 1

$$\Delta E^{(k)}(\{n\}) = \nu_k + 2\chi_{kk} + \frac{1}{2}\sum_{i\neq k}\chi_{ik} + 2\chi_{kk}n_k + \sum_{i\neq k}\chi_{ik}n_i \tag{3}$$

In the right-hand side of the above equation, the three first terms only depend on the mode k but not on its population. The last two terms, on the other hand, depend on the entire set of quantum numbers, including the couplings between mode k and all other modes $i \neq k$, and are the cause of the dependence of $\Delta E^{(k)}$ on $\{n\}$. On a side note, it should be mentioned that combination bands and overtones, which are not included in this model, could be added as well using a dedicated treatment.

Thermal equilibrium affects the distribution of quantum numbers, and hence the values of the transition energies, resulting in some shifting, broadening, or high-order effects. In the present model and as shown by eq 3, all of these features are directly related to anharmonicities and would of course vanish in the harmonic approximation.

To compute the absorption spectrum at fixed temperature, we first discretize a two-dimensional intensity histogram $\mathcal{S}(\nu,E)$ as a function of both the wavelength ν and the internal energy E. The Wang−Landau procedure already used for computing the microcanonical density of states provides the multicanonical weights needed to achieve flat-histogram sampling in energy space. We thus performed a second Monte Carlo simulation in the space of quantum numbers to build the accumulated absorption $\mathcal{S}(\nu,E)$ at wavelength ν and for a broad range of internal energies E as

$$\mathcal{S}(\nu, E) = \sum_{\text{MC steps}}\sum_{k}(n_k + 1)\sigma_{0\rightarrow 1}^{(k)}\delta[h\nu - \Delta E^{(k)}] \tag{4}$$

which upon normalizing by the number of entries $\mathcal{N}(\nu,E)$ in the histogram gives the microcanonical absorption intensity $I(\nu,E)$ as

$$I(\nu, E) = \frac{\mathcal{S}(\nu, E)}{\mathcal{N}(\nu, E)} \tag{5}$$

The multicanonical MC simulation also provides the distribution $\mathcal{P}_i(n_i,E)$ of vibrational quantum numbers for any given mode i as a function of internal energy. In the particular case of separable oscillators (harmonic or not), comparison can be made with the exact result

$$\frac{\mathcal{P}_i(n_i, E)}{\mathcal{P}_i(0, E)} = \frac{\Omega_i'(E - h\nu_i n_i)}{\Omega(E)} \tag{6}$$

where Ω_i' is the density of states of the set of oscillators excluding mode number i.

C. Absorption Spectrum at Finite Temperature. The absorption intensity $I(\nu,T)$ at finite temperature derives from the microcanonical quantity $I(\nu,E)$ by a standard Laplace transformation

$$I(\nu, T) = \frac{1}{Z}\int I(\nu, E)\Omega(E)\mathrm{e}^{-E/k_\mathrm{B}T}\mathrm{d}E \tag{7}$$

with Z as the partition function

$$Z(T) = \int \Omega(E)\mathrm{e}^{-E/k_\mathrm{B}T}\mathrm{d}E \tag{8}$$

More generally, this method provides the canonical properties at an arbitrary temperature by a single numerical integration and therefore allows averages and higher moments to be determined as a continuous function of temperature. This represents a drastic gain in computing cost with respect to scanning a temperature range by discretized steps and running direct simulations in the canonical ensemble.

III. Results and Discussion

We now apply the methods described in the previous section to the computation of absorption spectra of the naphthalene molecule in the infrared range, including finite temperature and anharmonic effects.

A. Calculation Details. The harmonic vibrational frequencies ν_i and anharmonic couplings χ_{ij} of naphthalene were taken from electronic structure calculations based on density functional theory, as recently reported by Cané et al.[79] All Monte Carlo simulations, including the Wang−Landau determination of the multicanonical weights and the multicanonical simulation themselves, used an energy grid of 1.24×10^{-2} eV. Twenty iterations were used for the Wang−Landau calculation, with an initial modification factor of $f = e$. A 90% flatness criterion was used at each iteration, with a maximum number of MC steps of 2×10^6. A higher accuracy was reached for the density of states $\Omega(E)$ by averaging the results of 100 independent calculations.

For the energy-dependent absorption spectra $I(\nu,E)$, the calculation was performed in the wavenumbers range of 0−3500 cm^{-1} with a binning of 0.1 cm^{-1}. This range is relevant for polycyclic aromatic hydrocarbons in the infrared domain, all of the fundamental frequencies falling within this energy range. The multicanonical Monte Carlo simulations carried out to compute $I(\nu,E)$ consisted of 6×10^8 MC steps.

B. Density of States and Thermal Distributions. The temperature range that is relevant for the present study is about 0−1500 K for naphthalene. As will be seen below, the internal energy range spanned by the molecule at the uppermost temperature lies up to about 6 eV above the zero-point vibrational energy. At this energy, investigations on cationic molecules[88–91] suggest that the dissociation rate remains very low compared to the infrared radiative cooling, even though the lowest fragmentation channel (H loss) is located at about 4.8 eV for this neutral molecule.[92] We also neglect stable isomers other than D_{2h} naphthalene. The fragmentation and isomerization phenomena cannot be described by the single Dunham expansion used here for the vibrational energy levels.

The variations of the microcanonical entropy $S(E)/k_\mathrm{B} = \ln \Omega(E)$ are shown in Figure 1a as a function of vibrational energy measured with respect to the zero-point energy. The values obtained for both the harmonic and coupled anharmonic systems are represented. As expected, they are close to each other in this low-energy range, the anharmonic entropy being slightly higher than the harmonic entropy. The entropies show smooth variations above 0.1 eV but stronger quantum fluctuations below this value.

The thermal energy distribution $P(E,T)$ was obtained from the density of states Ω at temperature T by Laplace transformation, $P(E,T) = \Omega(E)\exp(-E/k_\mathrm{B}T)/Z$. This distribution is illustrated in Figure 1b at $T = 350$ K. At this temperature, the

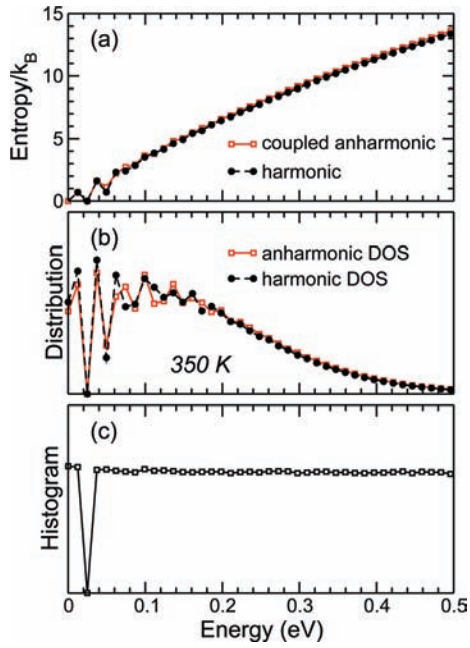

Figure 1. (a) Microcanonical entropy of the naphthalene molecule at low energy, assuming coupled anharmonic oscillators and obtained using a single Wang−Landau calculation in the broad energy range of $E \leq 6$ eV. The result obtained in the harmonic approximation by exact counting is also displayed. (b) Canonical probability distribution of internal energy at 350 K assuming coupled anharmonic or separable harmonic oscillators. (c) Histogram of energies visited during the multicanonical simulation. All energies are measured with respect to the zero-point level.

thermal distribution shows both the discontinuous, discrete character of the quantum density of states at low energies $E <$ 0.2 eV above the zero-point reference and a more continuous aspect at higher energies corresponding to the classical regime. In this figure, we also represented the thermal distribution obtained by assuming a harmonic density of states. The differences with the anharmonic calculation are rather small at such a low temperature but are clearly visible at internal energies lower than 0.2 eV.

The performance of the Wang−Landau method in achieving flat-histogram sampling in the space of quantum numbers is illustrated in Figure 1c, which shows the distribution obtained after the last WL iteration (modification factor $f \simeq 1 + 2^{-19}$). Except for one empty bin near 0.025 eV, the distribution is essentially uniform, with about 1.4% deviation with respect to the mean. The empty bin corresponds to energies that cannot be accommodated by any combination of quantum numbers and are thus unphysical for this system.

As the temperature is increased above 350 K, the sharp variations occurring at low energy of the thermal distribution become smoother. This transition to the classical regime is shown in Figure 2 for the temperatures of 500, 1000, and 1500 K. As in Figure 1b, we have quantified the extent of anharmonicity and coupling effects by showing the equivalent distributions obtained from the harmonic density of states. In addition to becoming smoother, the thermal distributions are progressively shifted toward higher energies, and they become broader. As mentioned previously, the upper energy range reached at 1500 K is about 6 eV. This indicates that higher temperatures should not be sampled with our scheme unless this energy limit is increased. Finally, the distributions obtained for the fully coupled system are further shifted to higher energies with respect to the harmonic calculation. At 1500 K, the shift

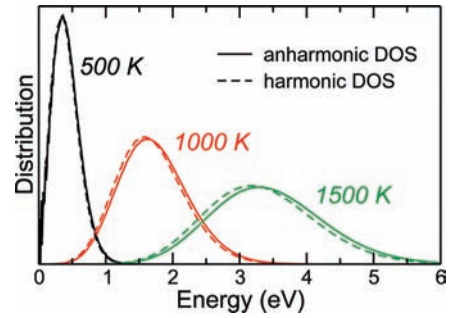

Figure 2. Normalized probability distributions of the internal energy of naphthalene, obtained from harmonic (dashed lines) and anharmonic (solid lines) microcanonical densities of states at thermal equilibrium at 500, 1000, and 1500 K. The energy is relative to the zero-point reference value.

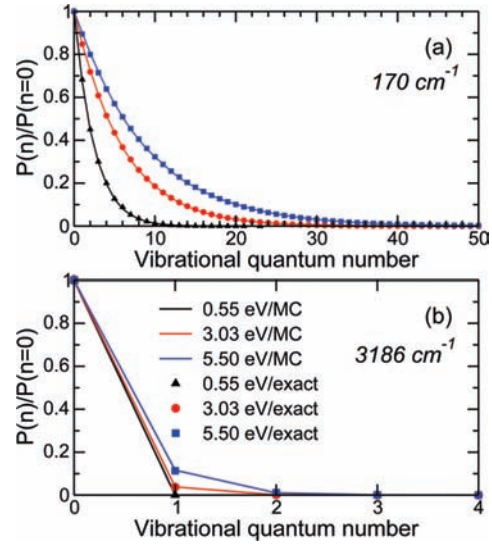

Figure 3. Distributions of vibrational quantum numbers for the naphthalene molecule at three internal energies of 0.55, 3.03, and 5.50 eV in the harmonic approximation. The two modes considered have harmonic frequencies of (a) 170 and (b) 3186 cm^{-1}. For all calculations, the numerical results obtained with the multicanonical Monte Carlo method are compared with the exact results from the Beyer−Swinehart algorithm.

reaches 0.11 eV at the maxima of the distributions, or an equivalent 3%.

C. Distributions of Vibrational Quantum Numbers. A necessary criterion for the calculated absorption spectra to be accurate is the ability to determine the distribution of vibrational quantum numbers, $\mathscr{P}_i(n_i,E)$, at microcanonical equilibrium. The performance of the multicanonical procedure to extract these distributions has been first checked in the harmonic case, for which the exact result of eq 6 applies. We show in Figure 3 the populations $\mathscr{P}_i(n_i,E)$ obtained for the stiffest ($\nu_i = 3186$ cm^{-1}) and the softest ($\nu_i = 170$ cm^{-1}) modes at three internal energies E. The multicanonical simulation was carried out using the numerical estimation of the harmonic density of states obtained with the Wang−Landau scheme, rather than that from the exactly known density.

For the two modes considered here, the numerical distributions found in the Monte Carlo simulations fully agree with the result of eq 6. This confirms the validity of our procedure for calculating not only the density of states but also the populations of quantum numbers that are essential for the absorption spectra.

In order to provide support for interpreting finite-temperature absorption spectra, anharmonic distributions of vibrational

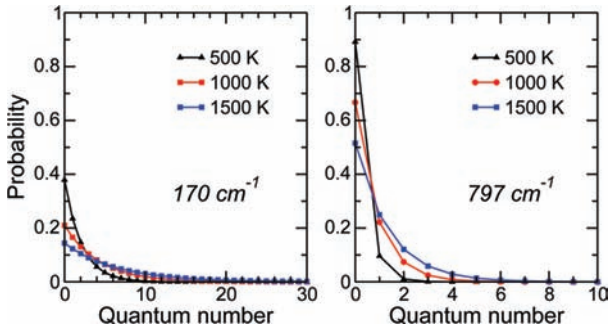

Figure 4. Distributions of vibrational quantum numbers for the naphthalene molecule at three temperatures for the modes with harmonic frequencies of 170 and 797 cm^{-1} and assuming full anharmonic couplings.

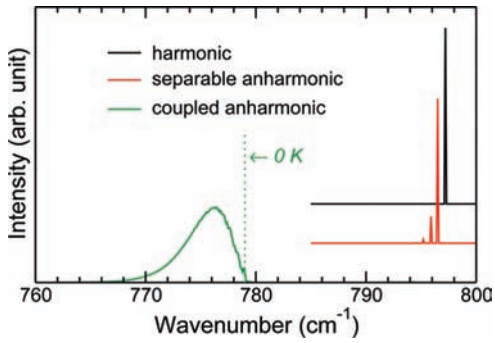

Figure 5. Absorption spectrum of the naphthalene molecule near 780 cm^{-1} at 500 K, obtained in the harmonic, separable anharmonic, and coupled anharmonic approximations. The vertical dotted line shows the location of the anharmonic frequency of this mode at 0 temperature. The three spectra have been vertically shifted to improve clarity.

quantum numbers have been calculated for thermalized systems using appropriate Laplace transformation of the microcanonical (anharmonic) distributions. We show in Figure 4 such distributions obtained at 500, 1000, and 1500 K for two modes discussed below in more detail, characterized by harmonic frequencies of 170 and 797 cm^{-1}, respectively. The thermal distributions display the expected decreasing shape with an exponential rate of about $h\nu_i/k_BT$ up to nontrivial anharmonic variations. Setting an arbitrary minimum population threshold of 10%, the softest mode is significantly populated by up to about 3 quanta at 500 K and 10 quanta at 1500 K. On the other hand, the stiffer mode near 800 cm^{-1} remains mainly in the ground vibrational state even at 1500 K. The harmonic distributions, which have been omitted from Figure 4 for a better readibility, look very similar, being only slightly narrower especially for the softer mode. While anharmonicities play a limited role in the equilibrium populations, their effect on the transition energies $\Delta E^{(k)}$ turns out to be more critical.

D. Absorption Spectra. The effects of various approximations in our calculated infrared absorption spectra are now discussed. Figure 5 displays the part of the spectrum associated with the out-of-plane C−H mode at $T = 500$ K. Three different calculations have been considered depending on the extent of anharmonicites. In the harmonic limit, a single peak is present at 797 cm^{-1}. A second calculation includes only the diagonal terms of the anharmonic matrix, the set of oscillators remaining separable. For this system, a sequence of peaks appears, corresponding to the hot bands that are separated by $2\chi_{kk} = -0.66$ cm^{-1} for this mode. The intensities of these peaks are related to the distributions of quantum numbers in the different vibrational states and also to the oscillator strength of the $n_k \rightarrow n_{k+1}$ transition. Finally, our third calculation includes the full

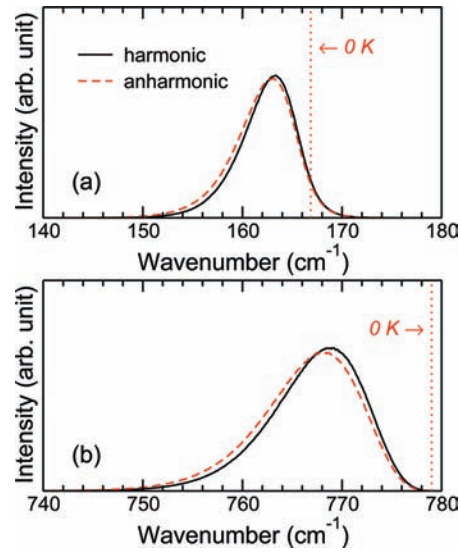

Figure 6. Absorption spectrum of the naphthalene molecule at 1000 K, obtained near (a) 170 and (b) 780 cm^{-1}, assuming anharmonic vibrational transitions. The density of states is taken from harmonic (solid lines) or coupled anharmonic (dashed lines) oscillators. The vertical dotted lines show the location of the anharmonic frequencies of these modes at 0 temperature.

anharmonic couplings in both the equilibrium populations and the transition energies. The peak strongly shifts to the red by more than 20 cm^{-1} and broadens significantly (width at midheight of 5 cm^{-1}). As mentionned, the red shift is the result of most anharmonic terms being negative. Broadening effects reflect the much larger diversity in the values of the transition energies, as well as the stronger dependence on the equilibrium population of quantum numbers.

It is useful to evaluate the separate contributions of anharmonicities to the transition energies and to the statistical distributions of quantum numbers at finite temperature. In this purpose, the absorption spectrum was calculated by assuming anharmonic transitions in eq 3, but with either the harmonic or fully anharmonic densities of states in eq 8. The results of these two calculations are illustrated in Figure 6 for the same two spectral regions close to 170 and 797 cm^{-1} at 1000 K. Figure 4 shows that this temperature has some quantitative influence on the equilibrium thermal distribution, the system lying in the ground vibrational state with a probability no greater than 22% for the softest mode or 65% for the stiffer mode. Remarkably, the harmonic approximation for the density of states has a very limited impact, with a small blue shift of about 0.7 cm^{-1} for both modes. Thus, the thermal broadening is essentially caused by the spreading of transition energies when anharmonicity is fully accounted for rather than being due to changes in the thermal population of vibrational quantum numbers.

Figure 7 further illustrates the predictions of our computational method for the absorption spectrum of naphthalene in two broader frequency regions, namely, 400−800 and 2900−3100 cm^{-1}, which correspond to those of the most infrared-active modes. The spectra shown correspond to the three temperatures of 500, 1000, and 1500 K. Both regions contain several peaks at low temperature. In the low-frequency region, the three vibrational bands generally display some red shifting and broadening with increasing temperature. We note however that the magnitude of these shifting and broadening effects varies depending on the mode. In particular, the mode near 480 cm^{-1} shifts only marginally. The higher-frequency domain corresponds to C−H stretchings and has two main bands at low

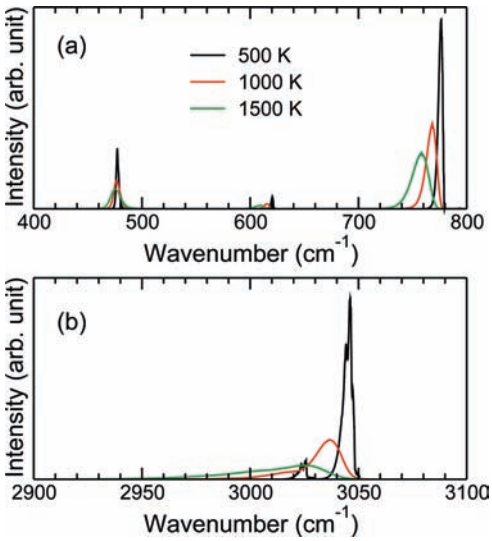

Figure 7. Absorption spectrum of the naphthalene molecule obtained at 500, 1000, and 1500 K using coupled anharmonic densities of states in two spectral regions, (a) 400−800 and (b) 2900−3100 cm^{-1}.

temperature separated by about 20 cm^{-1}. Interestingly, these bands broaden so much that they merge below 1000 K (not shown here) into a very asymmetric peak.

E. Temperature Effects on Spectral Features. We now consider the general features of the most intense absorption bands in terms of the three first moments $M^{(\alpha)}$ of the intensity $I(\nu,T)$. For a given band, the first and second moments, $M^{(1)}$ and $M^{(2)}$, provide the spectral shift and width, respectively denoted as $\langle\nu\rangle$ and $\Delta\nu$. The asymmetry of the band is characterized from the normalized third moment as a parameter γ such that

$$\gamma = \frac{M^{(3)}}{[M^{(2)}]^{3/2}} \tag{9}$$

With this definition, $\gamma \approx 0$ for a symmetric band, and $\gamma > 0$ (respectively, $\gamma < 0$) when the band profile is degraded to the blue (respectively, to the red). Obviously, the asymmetry parameter is only relevant if the band profile is not structured.

We have calculated the spectral shifts, widths, and asymmetries of the four most intense bands characterized by harmonic frequencies at 170, 482, 797, and 1030 cm^{-1} as a function of temperature in the range of 0−1500 K. These calculations were carried out using anharmonic densities of states and assuming anharmonic transition energies. The variations of $\langle\nu\rangle$ and $\Delta\nu$ with temperature are represented for these four modes in Figures 8 and 9, respectively.

The fundamental frequencies at 0 K are all shifted to the red with respect to the harmonic frequencies. As temperature increases, these four bands are generally further red shifted, except for the 482 cm^{-1} mode which shows a small blue shift at $T < 600$ K. This blue shift is related to the numerous positive anharmonic couplings between this mode and many other modes, especially the lowest-frequency mode at 170 cm^{-1}, as can be found from the appearance of a small additional peak shifted by +0.2 cm^{-1}, a value that matches the corresponding coupling of $\chi_{170,480} = +0.18$ cm^{-1}. Because the softest vibrational mode gets thermally populated first, the blue shift exhibited by the harmonic mode at 482 cm^{-1} is thus characteristic of positive anharmonic couplings with this softest vibration. The blue shift trend is further amplified by another

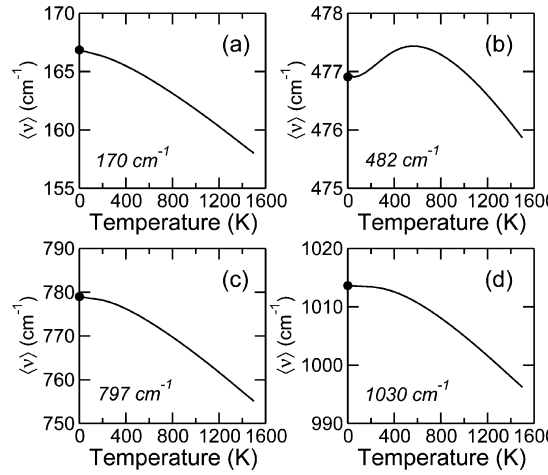

Figure 8. Variations with temperature of the spectral shift $\langle\nu\rangle$ of four vibrational bands for the naphthalene molecule, with harmonic frequencies at (a) 170, (b) 482, (c) 797, and (d) 1030 cm^{-1}. Note that the energy ranges spanned by the frequency shifts are different for each mode.

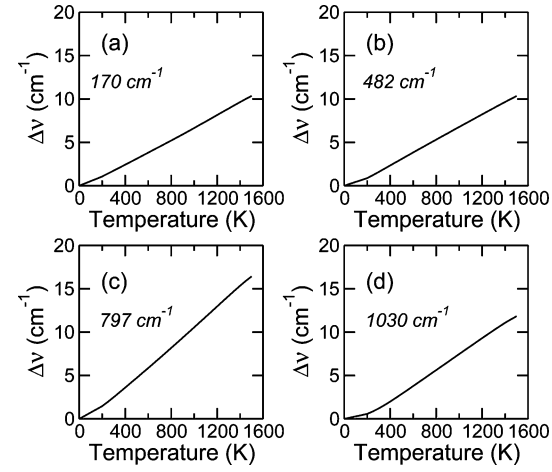

Figure 9. Variations with temperature of the spectral width $\Delta\nu$ of four vibrational bands for the naphthalene molecule, with harmonic frequencies at (a) 170, (b) 482, (c) 797, and (d) 1030 cm^{-1}.

positive coupling with the harmonic mode at 362 cm^{-1} (χ = +0.13 cm^{-1}).

Below 600 K, the three other modes in Figure 8a, c, and d exhibit some red shift, larger in magnitude than that for the 482 cm^{-1} mode. Looking at their anharmonic couplings with the softest mode and, consistently, with the observed behavior, the coefficients χ are all found to be negative, $\chi_{170,170} = -0.16$ cm^{-1}, $\chi_{170,797} = -0.66$ cm^{-1}, and $\chi_{170,1030} = -0.05$ cm^{-1}.

At higher temperatures, the contribution of the softest mode becomes less important as other modes become increasingly populated. Above $T = 800$ K, the variations of the spectral shift with temperature are essentially linear for the four modes, in agreement with experimental measurements performed for similar molecules.[43] The slope obtained for the most intense band at 797 cm^{-1} in the temperature range of 500−1000 K is about 1.8×10^{-2} cm^{-1} K^{-1}, which compares well with the values measured for pyrene (1.43×10^{-2} or 1.69×10^{-2} cm^{-1} K^{-1}) and coronene (1.61×10^{-2} or 2.30×10^{-2} cm^{-1} K^{-1}).[43] The two experimental values quoted here depend on the way the spectral positions of the vibrational bands were assigned as a function of temperature.[43]

In the C−H stretching spectral region, two vibrational bands are separated by about 20 cm^{-1} at temperatures below ap-

proximately 600 K. Above this value, the average spectral position also shows nearly linear decreasing variations (not shown here). The slope extracted between 600 and 900 K is found to be 2.5×10^{-2} cm^{-1} K^{-1}, comparable to the experimental values of 1.39×10^{-2} or 2.01×10^{-2} cm^{-1} K^{-1} obtained for naphthalene.[43] The slight discrepancy illustrates the difficulty to analyze properly C−H stretches in a region plagued with spectral congestion.

The evolution of the spectral widths versus temperature, shown in Figure 9, also reveals mainly linear variations for the four bands considered. The slopes obtained at temperatures in the range of 400−1200 K are about 6×10^{-3} cm^{-1} K^{-1} for the harmonic modes located at 170, 482, and 797 cm^{-1} and about 1.2×10^{-2} cm^{-1} K^{-1} for the harmonic mode at 797 cm^{-1}. Near 1000 K, the present work predicts the spectral widths to be around 5−10 cm^{-1}.

Next, the asymmetry parameter γ defined in eq 9 has been calculated as a function of temperature, but its variations are omitted for brevity. This parameter is generally found to be negative, with values close to −1 near 800 K, except for the mode at the harmonic frequency of 482 cm^{-1}, where $\gamma \approx 0.5$. The latter value emphasizes the importance of the positive intermode anharmonic coefficients for this particular out-of-plane C−C bending mode. In the experimental work of Joblin and co-workers,[43] the evolution of the spectral width has been mainly analyzed for pyrene, coronene, and ovalene, and linear behaviors were found in the three cases. However, the slopes extracted from these measurements were found to vary significantly with the molecular size due to the different numbers of vibrational transitions involved in a given spectral region. Hence, for these modes, it seems difficult to compare directly with the present calculations on naphthalene.

Experiments have also probed the C−H stretching modes, and the temperature dependence of the spectral features has been investigated specifically for naphthalene.[43] In the temperature range of 600−900 K, our calculations lead to a slope equal to 2.5×10^{-2} cm^{-1} K^{-1}, in semiquantitative agreement with the experimental value[43] of 3.53×10^{-2} cm^{-1} K^{-1}.

Finally, the rotational broadening $\Delta\nu_{rot}$ was not included in the present model, but it is important to assess its possible relevance. We have estimated this contribution to the spectral broadening in naphthalene based on the values for the rotational constants B determined by quantum chemistry calculations.[47] More precisely, $\Delta\nu_{rot}$ relates to B and the temperature T through $\Delta\nu_{rot} = 4(Bk_BT)^{1/2}$ (ref 93), or $\Delta\nu_{rot} \simeq 20$ cm^{-1} at $T = 1000$ K. This provides a lower bound for the actual accuracy that can be reached by the present theoretical description of pure anharmonic vibrations. Residual discrepancy with experiments may also be due to inaccuracies in the anharmonic matrix or the oscillator strengths for C−H stretching modes. Future progresses in density functional theory and computer hardware should enable the use of larger basis sets, which would significantly improve our description of the PES.

IV. Conclusions and Outlook

In this work, a novel method has been proposed to predict infrared absorption spectra of polyatomic molecules at finite temperature. Our theoretical scheme is based on three computational steps and relies on a second-order Dunham expansion for the vibrational energy levels as a parametric function of harmonic frequencies and an anharmonicity matrix. These ingredients are provided by quantum chemistry calculations, which, in the present case of naphthalene, were carried out by Cané and co-workers.[79] The absorption spectrum $I(\nu,T)$ is calculated in the canonical ensemble by Laplace transformation of the corresponding microcanonical quantity $I(\nu,E)$, that is, the absorption intensity as a function of internal energy and absorption wavelength, with the microcanonical density of states $\Omega(E)$. This quantity is obtained by a dedicated Wang−Landau Monte Carlo simulation, following rules described in a previous paper.[73] From the density of states, an additional flat-histogram MC simulation is carried out to record the absorption intensity $I(\nu,E)$ and, subsequently, the IR spectrum at arbitrary temperatures. The separation of the calculation into microcanonical stages allows the spectral features, including band shifts and band widths, to be characterized as a continuous function of temperature.

Application of the method to naphthalene has shown a generally good agreement with experimental data[43] for various modes in the temperature range of 500−900 K. In particular, the linear variations exhibited by both the spectral shift and broadening with temperature are well reproduced. The slopes are in semiquantitative correspondence with the measurements for the spectral shifts;[43] however, they are somewhat underestimated in the case of the broadenings. We interpreted this discrepancy as likely due to the neglect of rotational broadenings in the present calculation, and it would be useful to include these effects in our modeling. For this purpose, the rotational quantum numbers would have to be added as extra degrees of freedom, and rotational/vibrational couplings are expressed as additional terms in the energy function of eq 1. The contribution of combination bands and overtones could also be considered separately and added to the overall intensity histograms, provided that the corresponding absorption cross sections are properly estimated. The computational procedure for including these effects is essentially similar to the one presently used for elementary transitions, except that eq 3 should now be recalculated for each distinct transition. This could lead to a combinatorial increase in the simulation cost, unless the number of these transitions is a priori restricted. Work is currently in progress to include the effects of rotational/vibrational couplings, combination bands, and overtones.

Finally, the level of agreement between theory and experiment is obviously conditioned by the accuracy of the static ingredients, especially the anharmonicity coefficients. In the near future, advances in high-resolution FTIR spectroscopy on molecules of similar complexity should provide as many benchmarks for questioning this accuracy and hopefully for suggesting further improvements.

Acknowledgment. This work was supported by the French national programme "Physique et Chimie du Milieu Interstellaire" and the French "Agence Nationale de la Recherche" (Contract ANR-05-BLAN-0148-02). Financial support from GDR 2758 is gratefully acknowledged.

References and Notes

(1) Stoppa, P.; Pietropolli Charmet, A.; Tasinato, N.; Giorgianni, S.; Gambi, A. *J. Phys. Chem. A* **2009**, *113*, 1497.

(2) Asmis, K. R.; Pivonka, N. L.; Santambrogio, G.; Brümmer, M.; Kaposta, C.; Neumark, D. M.; Wöste, L. *Science* **2003**, *299*, 1375.

(3) Asmis, K. R.; Yang, Y.; Santambrogio, G.; Brümmer, M.; Roscioli, J. R.; McCunn, L. R.; Johnson, M. A.; Kühn, O. *Angew. Chem., Int. Ed.* **2007**, *46*, 8691.

(4) Asvany, O.; Kumar, P. P.; Redlich, B.; Hegemann, I.; Schlemmer, S.; Marx, D. *Science* **2005**, *309*, 1219.

(5) Zwier, T. S. *Annu. Rev. Phys. Chem.* **1996**, *47*, 205.

(6) Ebata, T.; Fujii, A.; Mikami, N. *Int. Rev. Phys. Chem.* **1998**, *17*, 331.

(7) Buck, U.; Huisken, F. *Chem. Rev.* **2000**, *100*, 3863.

(8) Wang, Y. S.; Tsai, C. H.; Lee, Y. T.; Chang, H. C.; Jiang, J. C.; Asvany, O.; Schlemmer, S.; Gerlich, D. *J. Phys. Chem. A* **2003**, *107*, 4217.
(9) Gruene, P.; Fielicke, A.; Meijer, G.; Janssens, E.; Ngan, V. T.; Nguyen, M. T.; Lievens, P. *ChemPhysChem* **2008**, *9*, 703.
(10) Gruene, P.; Rayner, D. M.; Redlich, B.; van der Meer, A. F. G.; Lyon, J. T.; Meijer, G.; Fielicke, A. *Science* **2008**, *321*, 674.
(11) Chapo, C. J.; Paul, J. B.; Provencal, R. A.; Roth, K.; Saykally, R. J. *J. Am. Chem. Soc.* **1998**, *120*, 12956.
(12) Snoek, L. C.; Kroemer, R. T.; Hockridge, M. R.; Simons, J. P. *Phys. Chem. Chem. Phys.* **2001**, *3*, 1819.
(13) Dian, B. C.; Zwier, T. S. *Science* **2004**, *303*, 1169.
(14) Kapota, C.; Lemaire, J.; Maître, P.; Ohanessian, G. *J. Am. Chem. Soc.* **2004**, *126*, 1836.
(15) Jurchen, J. C.; Garcia, D. E.; Williams, E. R. *J. Am. Mass Spectrom.* **2004**, *14*, 1373.
(16) Choi, M. Y.; Miller, R. E. *J. Am. Chem. Soc.* **2006**, *128*, 7320.
(17) Bakker, J. M.; Compagnon, I.; Meijer, G.; von Helden, G.; Kabelac, M.; Hobza, P.; de Vries, M. S. *Phys. Chem. Chem. Phys.* **2004**, *6*, 2810.
(18) Chin, W.; Piuzzi, I. F.; Dimicoli, I.; Mons, M. *Phys. Chem. Chem. Phys.* **2006**, *8*, 1033.
(19) Compagnon, I.; Oomens, J.; Meijer, G.; von Helden, G. *J. Am. Chem. Soc.* **2006**, *128*, 3592.
(20) Brenner, J. D.; Barker, J. R. *Astrophys. J.* **1992**, *388*, L39.
(21) Schlemmer, S.; Cook, D. J.; Harrison, J. A.; Wurfel, B.; Chapman, W.; Saykally, R. J. *Science* **1994**, *265*, 1686.
(22) Williams, R. M.; Leone, S. R. *Astrophys. J.* **1995**, *443*, 675.
(23) Cook, D. J.; Schlemmer, S.; Balucani, N.; Wagner, D. R.; Steiner, B.; Saykally, R. J. *Nature (London)* **1996**, *380*, 227.
(24) Wagner, D. R.; Kim, H. S.; Saykally, R. J. *Astrophys. J.* **2000**, *545*, 854.
(25) Kim, H.-S.; Wagner, D. R.; Saykally, R. J. *Phys. Rev. Lett.* **2001**, *86*, 5691.
(26) Kim, H.-S.; Saykally, R. J. *Astrophys. J., Suppl. Ser.* **2002**, *143*, 455.
(27) Piest, H.; von Helden, G.; Meijer, G. *Astrophys. J. Lett.* **1999**, *520*, L75.
(28) Oomens, J.; van Roij, A. J. A.; Meijer, G.; von Helden, G. *Astrophys. J.* **2000**, *542*, 404.
(29) Oomens, J.; Sartakov, B. G.; Tielens, A. G. G. M.; Meijer, G.; von Helden, G. *Astrophys. J. Lett.* **2001**, *560*, L99.
(30) Oomens, J.; Tielens, A. G. G. M.; Sartakov, B. G.; von Helden, G.; Meijer, G. *Astrophys. J.* **2003**, *591*, 968.
(31) Pirali, O.; Van-Oanh, N.-T.; Parneix, P.; Vervloet, M.; Bréchignac, Ph. *Phys. Chem. Chem. Phys.* **2006**, *8*, 3707.
(32) Pirali, O.; Mulas, G.; Malloci, G.; Vervloet, M.; Tokaryk, D. W.; Oomens, J.; Joblin, C. In *Molecules in Space and Laboratory*; Lemaire, J.-L., Combes, F., Eds.; 2008.
(33) Lorenz, U. J.; Solca, N.; Lemaire, J.; Maître, P.; Dopfer, O. *Angew. Chem., Int. Ed.* **2007**, *46*, 6714.
(34) Richter, H.; Howard, J. B. *Prog. Energy Combust. Sci.* **2000**, *265*, 26.
(35) Reilly, P. T. A.; Gieray, R. A.; Whitten, W. V.; Ramsey, J. M. *Combust. Flame* **2000**, *122*, 90.
(36) Tielens, A. G. G. M. *Annu. Rev. Astron. Astrophys.* **2008**, *46*, 289.
(37) Puget, J. L.; Léger, A. *Anun. Rev. Astron. Astrophys.* **1989**, *27*, 161.
(38) Allamandola, L. J.; Tielens, A.; G, G. M.; Barker, J. R. *Astrophys. J., Suppl. Ser.* **1989**, *71*, 733.
(39) Léger, A.; Puget, J. *Astron. Astrophys.* **1984**, *137*, L5.
(40) Allamandola, L.; Tielens, A.; Barker, J. *Astrophys. J. Lett.* **1985**, *290*, L25.
(41) Shan, J.; Suto, M.; Lee, L. C. *Astrophys. J.* **1991**, *383*, 459.
(42) van Heijnsbergen, D.; von Helden, G.; Sartakov, B.; Meijer, G. *Chem. Phys. Lett.* **2000**, *321*, 508.
(43) Joblin, C.; Boissel, P.; Léger, A.; d'Hendecourt, L.; Défourneau, D. *Astron. Astrophys.* **1995**, *299*, 835.
(44) Cook, D. J.; Saykally, R. J. *Astrophys. J.* **1998**, *493*, 793.
(45) Pech, C.; Joblin, C.; Boissel, P. *Astron. Astrophys.* **2002**, *388*, 639.
(46) Joblin, C.; Toublanc, D.; Boissel, P.; Tielens, A. G. G. M. *Mol. Phys.* **2002**, *100*, 3595.
(47) Mulas, G.; Malloci, G.; Joblin, C.; Toublanc, D. *Astron. Astrophys.* **2006**, *456*, 161.
(48) Merrick, J. P.; Moran, D.; Radom, L. *J. Phys. Chem. A* **2007**, *111*, 11683.
(49) Schultheis, V.; Reichold, R.; Schropp, B.; Tavan, P. *J. Phys. Chem. B* **2008**, *112*, 12217.
(50) Van-Oanh, N.-T.; Parneix, P.; Bréchignac, Ph. *J. Phys. Chem. A* **2002**, *106*, 10144.
(51) Van-Oanh, N.-T.; Parneix, P.; Bréchignac, Ph. *Phys. Chem. Chem. Phys.* **2005**, *7*, 1779.
(52) Kumar, P. P.; Marx, D. *Phys. Chem. Chem. Phys.* **2006**, *5*, 573.
(53) Rega, N. *Theor. Chem. Acc.* **2006**, *116*, 347.
(54) Estácio, S. G.; Costa Cabral, B. J. *Chem. Phys. Lett.* **2008**, *456*, 170.
(55) Ramírez, R.; López-Ciudad, T.; Kumar, P. P.; Mark, D. *J. Chem. Phys.* **2004**, *121*, 3973.
(56) Shiga, M.; Nakayama, A. *Chem. Phys. Lett.* **2007**, *451*, 175.
(57) Kaczmarek, A.; Shiga, M.; Marx, D. *J. Phys. Chem. A* **2009**, *113*, 1985.
(58) Jung, J. O.; Gerber, R. B. *J. Phys. Chem.* **1996**, *105*, 10332.
(59) Matsunaga, N.; Chaban, G. M.; Gerber, R. B. *J. Chem. Phys.* **2002**, *117*, 3541.
(60) Signorell, R. *J. Chem. Phys.* **2003**, *118*, 2707.
(61) Beyer, T.; Swinehart, D. *Commun. ACM* **1973**, *16*, 379.
(62) Stein, S.; Rabinovitch, B. *J. Chem. Phys.* **1973**, *58*, 2438.
(63) (a) Doll, J. D. *Chem. Phys. Lett.* **1980**, *72*, 139. (b) Berblinger, M.; Schlier, C. *J. Chem. Phys.* **1992**, *96*, 6834.
(64) Parneix, P.; Van-Oanh, N.-T.; Bréchignac, Ph. *Chem. Phys. Lett.* **2002**, *357*, 78.
(65) Börjesson, L. E. B.; Nordholm, S.; Andersson, L. A. *Chem. Phys. Lett.* **1991**, *186*, 65. (a) Krems, R.; Nordholm, S. *Z. Phys. Chem.* **2000**, *214*, 1467.
(66) Wadi, H.; Pollak, E. *J. Chem. Phys.* **1999**, *110*, 8246.
(67) Romanini, D.; Lehmann, K. K. *J. Chem. Phys.* **1993**, *98*, 6437.
(68) (a) Noid, D. W.; Koszykowski, M. L.; Tabor, M.; Marcus, R. M. *J. Chem. Phys.* **1980**, *72*, 6169. (b) Farantos, S. C.; Murrel, J. N.; Hajduk, J. C. *Chem. Phys.* **1982**, *68*, 109.
(69) (a) Barker, J. R. *J. Phys. Chem.* **1987**, *91*, 3849. (b) Toselli, B. M.; Barker, J. R. *Chem. Phys. Lett.* **1989**, *159*, 499.
(70) Hüpper, B.; Pollak, E. *J. Chem. Phys.* **1999**, *110*, 11176.
(71) (a) Wang, F.; Landau, D. P. *Phys. Rev. Lett.* **2001**, *86*, 2050 (2001). (b) Wang, F.; Landau, D. P. *Phys. Rev. E* **2001**, *64*, 056101.
(72) Dayal, P.; Trebst, S.; Wessel, S.; Würtz, D.; Troyer, M.; Sabhapandit, S.; Coppersmith, S. N. *Phys. Rev. Lett.* **2004**, *92*, 097201.
(73) Basire, M.; Parneix, P.; Calvo, F. *J. Chem. Phys.* **2008**, *129*, 081101.
(74) Szczepanski, J.; Vala, M. *Astrophys. J.* **1993**, *414*, 655.
(75) Hudgins, D. M.; Sandford, S. A.; Allamandola, L. J. *Astrophys. J.* **1994**, *98*, 4242.
(76) Miller, M. D.; Talbi, D.; Pauzat, F.; Ellinger, Y. *Astrophys. J.* **1993**, *408*, 530.
(77) Pauzat, F.; Talbi, D.; Ellinger, Y. *Astron. Astrophys.* **1995**, *293*, 263.
(78) Langhoff, S. R. *J. Phys. Chem.* **1996**, *100*, 2819.
(79) Cané, E.; Miani, A.; Trombetti, A. *J. Phys. Chem. A* **2007**, *111*, 8218.
(80) Barone, V. *J. Chem. Phys.* **2005**, *122*, 014108.
(81) Zhou, C.; Bhatt, R. N. *Phys. Rev. E* **2005**, *72*, 025701.
(82) Jayasri, D.; Sastry, V. S. S.; Murthy, K. P. N. *Phys. Rev. E* **2005**, *72*, 036702.
(83) Zhou, C.; Shulthess, T. C.; Torbrügge, S.; Landau, D. P. *Phys. Rev. Lett.* **2006**, *96*, 120201.
(84) Poulain, P.; Calvo, F.; Antoine, R.; Broyer, M.; Dugourd, P. *Phys. Rev. E* **2006**, *73*, 056704.
(85) Khan, M. O.; Kennedy, G.; Chan, D. Y. C. *J. Comput. Chem.* **2005**, *26*, 72.
(86) Belardinelli, R. E.; Pereyra, V. D. *J. Chem. Phys.* **2007**, *127*, 184105.
(87) Zhan, L. *Comput. Phys. Commun.* **2008**, *179*, 339.
(88) Rühl, E.; Price, S. D.; Leach, S. *J. Phys. Chem.* **1989**, *93*, 6312.
(89) Jochims, H. W.; Rühl, E.; Baumgartel, H.; Leach, S. *Chem. Phys.* **1992**, *168*, 159.
(90) Ho, Y.-P.; Dunbar, R. C.; Lifshitz, C. *J. Am. Chem. Soc.* **1995**, *117*, 6504.
(91) Pino, T.; Parneix, P.; Calvo, F.; Bréchignac, Ph. *J. Phys. Chem. A* **2007**, *111*, 4456.
(92) Bauschlicher, C. W.; Langhoff, S. R. *Mol. Phys.* **1999**, *96*, 471.
(93) Le Coupanec, P.; Rouan, D. *Astron. Astrophys.* **1998**, *338*, 217.

JP901104X